

Interacting dark matter contribution to the Galactic 511 keV gamma ray emission: constraining the morphology with INTEGRAL/SPI observations

Aaron C. Vincent^{*,1}, Pierrick Martin^{†,2} and James M. Cline^{‡1}

¹*Department of Physics, McGill University, 3600 Rue University, Montréal, Québec, Canada H3A 2T8*

²*Institut de Planétologie et d'Astrophysique de Grenoble, BP 53, 38041 Grenoble cedex 9, France*

We compare the full-sky morphology of the 511 keV gamma ray excess measured by the INTEGRAL/SPI experiment to predictions of models based on dark matter (DM) scatterings that produce low-energy positrons: either MeV-scale DM that annihilates directly into e^+e^- pairs, or heavy DM that inelastically scatters into an excited state (XDM) followed by decay into e^+e^- and the ground state. By direct comparison to the data, we find that such explanations are consistent with dark matter halo profiles predicted by numerical many-body simulations for a Milky Way-like galaxy. Our results favor an Einasto profile over the cusper NFW distribution and exclude decaying dark matter scenarios whose predicted spatial distribution is too broad. We obtain a good fit to the shape of the signal using six fewer degrees of freedom than previous empirical fits to the 511 keV data. We find that the ratio of flux at Earth from the galactic bulge to that of the disk is between 1.9 and 2.4, taking into account that 73% of the disk contribution may be attributed to the beta decay of radioactive ^{26}Al .

1. INTRODUCTION

The 511 keV gamma ray line observed by the INTEGRAL/SPI experiment is consistent with the annihilation of $\sim (1.5 \pm 0.1) \times 10^{43}$ low-energy positrons per second in a region within ~ 1 kpc of the galactic center (GC), in addition to a fainter $((0.3 \pm 0.2) \times 10^{43} e^+ s^{-1})$ disk-like component that extends along the galactic plane [1]. The line is mostly due to parapositronium annihilation of thermal or near-thermal positrons [2, 3]. The absence of γ rays from e^+ annihilations in flight implies that the positrons are injected with energies less than ~ 3 MeV [4]. No astrophysical source has been proven to yield such positrons with the required concentrated and approximately axially symmetric spatial distribution.

Among conventional sources, radioactive ejecta from stars, supernovae and gamma-ray bursts can produce a large enough rate of positrons through β^+ decay, but their spatial distribution is not sufficiently confined toward the bulge: they predict a ratio of bulge to disk luminosities $B/D < 0.5$, whereas observations demand $B/D > 1.4$. Other proposed mechanisms also suffer from this problem. In addition, positrons from pair creation near pulsars or from $p-p$ collisions associated with cosmic rays or the supermassive black hole tend to be too energetic. Low-mass X-ray binaries have received attention as a possible source, but these also do not give rise to large enough B/D [5]. A comprehensive review of these sources and the challenges they face is given in [6].

Dark matter (DM) interactions have the potential to explain the observed excess, either through direct annihilations of light (\sim few MeV) DM particles into e^+e^- pairs [7], or by the excited dark matter (XDM) mechanism, in

which excited states of heavy DM (χ) are produced in $\chi-\chi$ collisions, with subsequent decay of the excited state into the ground state and an e^+e^- pair [8, 9]. The latter scenario has the theoretical advantage that the DM mass is relatively unconstrained, requiring only that the splitting between the ground and excited states be less than a few MeV.

XDM as an explanation for the INTEGRAL/SPI 511 keV excess came under greater scrutiny in recent years after it was proposed [10] that nonabelian DM models could naturally have small \sim MeV mass splittings and simultaneously explain additional recent cosmic ray anomalies [11, 12] as well as hints of direct DM detection [13]. Ref. [14] found that it is not possible to get a large enough rate of positrons for 511 keV emission in the nonabelian models that require production of *two* e^+e^- pairs (one at each interaction vertex). However, the original model of [8] can give a large enough rate [15] since only one such pair need be produced, which is energetically easier. Moreover, variant models involving metastable DM that scatters through a smaller mass gap [16, 17] also give a large enough rate, and are largely free of threshold velocity issues.

The aforementioned studies focused primarily on matching the overall rate of positron production, either ignoring morphological constraints or estimating them in a rough way. Ref. [18] is the only rigorous analysis with respect to dark matter models, done at a time when relatively little data had yet been accumulated. More recently, ref. [19] carried out a study of DM predictions for the 511 keV angular profile, but comparing to a previous fit to the observed shape [20] rather than directly to the data.

Our purpose in the present work is to improve upon these earlier papers by testing the DM model shape predictions directly against the most recent INTEGRAL data. We will then examine how these DM models compare to the phenomenological models obtained in previous studies, such as [21, 22], where the 511 keV celestial

*vincenta@hep.physics.mcgill.ca

†pierrick.martin@obs.ujf-grenoble.fr

‡jcline@hep.physics.mcgill.ca

signal is represented by analytical shape functions with several free parameters. As we will see, an interesting feature of the DM models is that their predictions depend on far fewer parameters and they can thus be a more attractive candidate if they are shown to provide as good a fit as the phenomenological parametrizations.

In the remainder of the paper, we first present the known sources of positrons in the galaxy, before discussing our procedure for modeling the 511 keV sky in Sections 3 and 4. We give our main results, along with the details of our fitting procedure, in Section 5 and briefly discuss the implications of this study in Section 6.

2. KNOWN BACKGROUNDS

In order to correctly model the possible contribution to the 511 keV signal from DM scattering, it is necessary to subtract from the data the contributions from known sources of low-energy positrons. They can be produced from β^+ decay of ^{26}Al expelled from massive stars, as well as from ^{44}Ti and ^{56}Ni produced in supernovae. These contributions should be correlated with the stars in the galaxy, thus contributing dominantly to the disk component of the observed signal.

The contribution of ^{26}Al can be more directly assessed than that of the other radio-isotopes. During ^{26}Al decay, the de-excitation of the resulting ^{26}Mg nucleus produces a gamma ray signal at an energy of 1809 keV whose magnitude and morphology has also been mapped by INTEGRAL/SPI [23]. Since each decay produces a positron and an 1809 keV photon, one can unambiguously determine the fraction of the 511 keV signal originating from ^{26}Al . Ref. [1] showed that it accounts for roughly half of the disk component of the 511 keV signal, and we will confirm this. The contribution of ^{44}Ti and ^{56}Ni positrons cannot be evaluated in that way because of their shorter lifetimes. A corollary is that positron escape from supernova and their remnants can be a serious issue, and prevent the determination of positron injection rate directly from the isotopes yields [24, 25]. Estimates of the isotopes production in stars and of positron escape fractions suggest that it should make up most of the remaining disk emissivity [1, 6].

3. DARK MATTER HALO PROFILE

Many-body simulations of the formation of galactic halos by collapsing dark matter particles predict a triaxial halo (see for example [26]), which however becomes more approximately spherical near the galactic center when the effects of baryons are taken into account [27]. For simplicity we will consider the halos to be spherically symmetric in most of the present work, although we will show that adding a realistic degree of oblateness does not significantly alter the fit. To further constrain the shape of the halo we will refer to results of the *Via Lactea II*

simulation [28], which modeled the collapse of a Milky Way-sized ($2 \times 10^{12} M_\odot$) collection of over 10^9 particles. We chose *Via Lactea II* because it was specifically geared towards the study of the dark matter halo of the Milky Way. Among the many known parametrizations of the radial mass-energy density distribution, two have been especially successful at parametrizing results of recent simulations. These are the Einasto profile

$$\rho(r) = \rho_s \exp\left(-\left[\frac{2}{\alpha}\left(\frac{r}{r_s}\right)^\alpha - 1\right]\right) \quad (1)$$

and the generalized Navarro-Frenk-White (NFW) profile,

$$\rho(r) = \rho_s \frac{2^{3-\gamma}}{(r/r_s)^\gamma (1+r/r_s)^{3-\gamma}}. \quad (2)$$

In both cases r is the galactocentric radius, while r_s , α and γ are parameters fit to N-body simulation results. The main galactic halo of the *Via Lactea II* simulation may be fit to an Einasto profile with $r_s = 25.7$ kpc and $\alpha = 0.17$, or to an NFW profile with $r_s = 26.2$ kpc and a central slope of $\gamma = 1.2$ [29]. The overall density normalization ρ_s can be computed from the local dark matter density which we take to be $\rho_\odot = 0.4 \text{ GeV cm}^{-3}$ [30] at the sun's position $r_\odot = 8.5$ kpc [31].

4. DM AND THE 511 KEV SKY DISTRIBUTION

Although the decaying DM scenario [32] was already shown to be highly disfavored in refs. [18, 19], for completeness we will retest it in the present work. The flux of 511 keV photons from an e^+ produced in the decay of a metastable DM particle χ of mass m_χ is

$$d\Phi = 2(1 - 0.75f_p) \frac{d\Omega}{4\pi} \int_{l.o.s.} \frac{\rho(\ell)}{m_\chi \tau} d\ell \quad (3)$$

The integral is along the observer's line of sight parametrized by ℓ , τ is the lifetime, $\rho(\ell)$ is its position-dependent density and $f_p = 0.967 \pm 0.022$ is the positronium fraction [3]. It corresponds to the global probability that a given e^+e^- annihilation take place via positronium formation. The latter can occur in the triplet state ortho-positronium (o-Ps) or the singlet state para-positronium (p-Ps). To conserve angular momentum, only p-Ps may decay into two 511 keV photons.

If the positrons are instead produced in a scattering or annihilation event, the observed flux takes a similar form:

$$d\Phi = 2(1 - 0.75f_p) \frac{d\Omega}{4\pi} \int_{l.o.s.} \frac{1}{2} \frac{\langle\sigma v\rangle \rho^2(\ell)}{m_\chi^2} d\ell \quad (4)$$

where $\langle\sigma v\rangle$ is the thermally averaged cross-section for annihilations or excitations of the DM particles that produce e^+e^- pairs. Henceforth we will use "scattering" as shorthand for either XDM scattering or annihilating

light DM, since both processes will look like (4) to an observer. The density-squared dependence of this integral means that the observed flux is much more concentrated in the galactic center than in the decay case; this is why scattering gives a much better fit to the observed shape than do decays.

The forms (3,4) are only strictly correct if positrons annihilate close to where they were formed. Despite recent studies [33, 34] the problem of positron transport in the interstellar medium cannot be considered as fully settled. In the absence of strong theoretical and observational constraints, we will assume that positron transport is a small effect in the present investigation. We will briefly return to this issue in Section 6.

Moreover, we have for simplicity assumed that $\langle\sigma v\rangle$ in (4) is independent of r , but this is not a good approximation for all models. In particular, for the standard XDM scenarios with a total energy gap $\delta E > 0$ between the ground state and excited state(s), there is a threshold value for the relative velocity, $v_t = 2\sqrt{\delta E/m_\chi}$, which appears in the excitation cross section as $\sigma v \sim \sigma_0\sqrt{v^2 - v_t^2}$ [8]. Because the DM velocity dispersion $v_0(r)$ depends strongly upon r near the galactic center, this factor can then introduce significant r dependence into the phase-space average $\langle\sigma v\rangle$. There are several situations where this is not important: MeV DM undergoing pure annihilations [7, 35], metastable XDM models where $\delta E \ll m_e$ or $\delta E < 0$ [14, 17], and standard XDM models where $m_\chi \gtrsim \text{TeV}$, in which case v_t is small compare to $v_0(r)$. For XDM models with $m_\chi \lesssim \text{TeV}$, a more detailed study should be done.

In addition to the dark matter source of positrons, we included a disk component that models β^+ emission from radioactive isotopes including ^{26}Al and ^{44}Ti , whose flux at earth is analogous to eq. (3); the combination $\rho/(m_\chi\tau)$ becomes a density per unit time \dot{n} of positron-producing radioactive decays. We considered two density models for this component. The first is a Robin young stellar disk (YD) model [1, 36],

$$\dot{n}_{YD}(x, y, z) = \dot{n}_0 \left[e^{-\left(\frac{a}{R_0}\right)^2} - e^{-\left(\frac{a}{R_i}\right)^2} \right], \quad (5)$$

with

$$a^2 = x^2 + y^2 + z^2/\epsilon^2. \quad (6)$$

The fixed disk scale radius is $R_0 = 5$ kpc and the fixed inner disk truncation radius is $R_i = 3$ kpc. We varied the vertical height scale $z_0 = \epsilon/R_0$ between 50 pc and 140 pc. (Ref. [23] used the 1809 keV line to fit the ^{26}Al distribution to a YD distribution with $z_0 = 125$ pc.) For comparison we also took an old disk (OD) model:

$$\dot{n}_{OD}(x, y, z) = \dot{n}_0 \left[e^{-\left(0.25 + \frac{a^2}{R_0^2}\right)^{1/2}} - e^{-\left(0.25 + \frac{a^2}{R_i^2}\right)^{1/2}} \right], \quad (7)$$

with $R_0 = 2.53$ kpc, $R_i = 1.32$ kpc and a vertical height scale z_0 which was varied from 150 to 250 pc.

5. RESULTS

We tested our DM scenario against the INTEGRAL/SPI data by a model-fitting procedure applied to about 8 years of data collected in an energy bin of 5 keV width centered around 511 keV. For this, a model for the sky emission is convolved by the instrument response function and fitted to the data simultaneously to a model for the instrumental background noise in the Ge detectors.

Our fitting procedure is the same as the one described in section 4.2.1 of [1]. The likelihood L of a model assuming a Poisson distribution of events in each of the N data bins is

$$L = \prod_{i=1}^N \frac{\lambda_i^{n_i} e^{-\lambda_i}}{n_i!}. \quad (8)$$

n_i is the number of events recorded in bin i by the SPI experiment, and $\lambda_i = \sum_k \alpha_k s_i^k + b_i(\beta)$ is the predicted number of counts per bin, including the background b_i and the source $s_i^k = \sum_j f_j^k R_i^j$. The factor R_i^j is the instrument response matrix and f_j^k is the intensity computed with the line-of-sight integrals. In our case, the sum over k has two terms: the dark matter term and the disk component. The coefficients α_k and β are the scaling factors that are adjusted by the fit. The result of fixing the normalization α_{DM} is to fix $(m_\chi\tau_\chi)^{-1}$ in the case of decay and $\langle\sigma v\rangle_\chi m_\chi^{-2}$ for dark matter scattering. We use the maximum likelihood ratio test to estimate detection significances and errors. We calculate the log-likelihood ratio

$$\text{MLR} = -2(\ln L_0 - \ln L_1), \quad (9)$$

where L_1 is the maximized likelihood of the model being tested, and L_0 is the maximum likelihood of the background model only, *i.e.*, $\alpha_k = 0$.

We compare the results of our DM models to the phenomenological description by Weidenspointner *et al.* [21], where the authors fitted two spheroidal Gaussians and a young stellar disk to the then-available four-year data set¹. We have updated their analysis, using the currently available eight-year data set and find an MLR of 2693. Although non-nested models cannot be directly compared through the MLR, this serves as a the figure of merit for a model such as the dark matter ones to match, if it is to provide a competitive fit relative to the phenomenological shape models.

We performed two analyses, firstly fixing α and r_s to values favored by *Via Lactea II*, using the young disk model parameters favored by the ^{26}Al analysis of [23], and

¹ The 8 degrees of freedom in the reference model are: the width and normalization of each Gaussian, the inner and outer disk truncation, the disk scale height and the disk normalization.

Table I: Summary of best fits to the INTEGRAL/SPI data, with parameters fixed to results of the *Via Lactea II* simulation. This corresponds to $r_s = 26$ kpc and $\alpha = 0.17$ for an Einasto profile (1) or $\gamma = 1.2$ for an NFW profile (2). The disk component is the young disk (5) with $z_0 = 125$ pc. All-sky fluxes are in units of 10^{-4} ph cm $^{-2}$ s $^{-1}$, the lifetimes τ are in seconds, and cross-sections $\langle\sigma v\rangle$ have units of cm 3 s $^{-1}$. We have highlighted the best fit scenarios in bold.

Channel	Profile	MLR	Disk flux	DM flux	DM lifetime or cross-section
decay	Einasto only	2139	—	174.5 ± 3.5	$\tau_\chi = 1.1 \times 10^{26} (\text{GeV}/m_\chi)$
	Einasto + Disk	2194	10.60 ± 1.42	148.6 ± 5.1	$\tau_\chi = 1.3 \times 10^{26} (\text{GeV}/m_\chi)$
scattering	Einasto only	2611	—	24.02 ± 0.47	$\langle\sigma v\rangle_\chi = 5.8 \times 10^{-25} (m_\chi/\text{GeV})^2$
	Einasto + Disk	2668	9.98 ± 1.32	21.16 ± 0.59	$\langle\sigma v\rangle_\chi = 5.1 \times 10^{-25} (m_\chi/\text{GeV})^2$
	Einasto (oblate) + Disk	2669	8.74 ± 1.31	21.06 ± 0.61	$\langle\sigma v\rangle_\chi = 4.9 \times 10^{-25} (m_\chi/\text{GeV})^2$
	NFW only	1602	—	6.72 ± 0.17	$\langle\sigma v\rangle_\chi = 8.2 \times 10^{-26} (m_\chi/\text{GeV})^2$
	NFW + Disk	2155	26.45 ± 1.25	4.90 ± 0.18	$\langle\sigma v\rangle_\chi = 6.1 \times 10^{-26} (m_\chi/\text{GeV})^2$

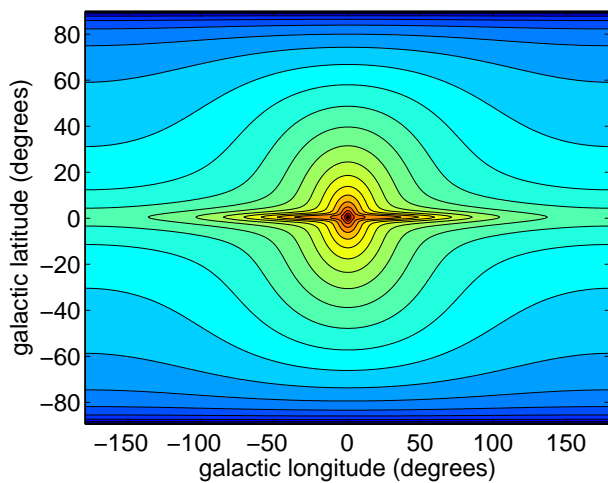


Figure 1: Intensity skymap predicted by *Einasto + disk* model. The bulge component is due to emission from scattering or annihilating dark matter in an Einasto profile, and the disk component can be attributed to decay of radioactive species including mainly ^{26}Al .

finding the overall normalizations of the disk and Einasto components that best fit the INTEGRAL/SPI data. As a second analysis, we varied the parameters α and r_s of the Einasto profile, as well as the height scales z_0 for both young and old disk populations. As we will show, adding these three extra degrees of freedom does not significantly improve the likelihood of the model, suggesting that the *Via Lactea II* parameters are a good fit for the scattering XDM or annihilating DM hypothesis.

Table I summarizes our main results. The dark matter halo parameters were set to those favored by *Via Lactea II*, for an Einasto (NFW) profile with $r_s = 26$ kpc and $\alpha = 0.17$ ($\gamma = 1.2$). We used the young disk model (5) of [23], with the fixed scale height $z_0 = 125$ pc corresponding to the ^{26}Al distribution inferred from 1809 keV line data. We considered both decaying (3) and scattering (4) dark

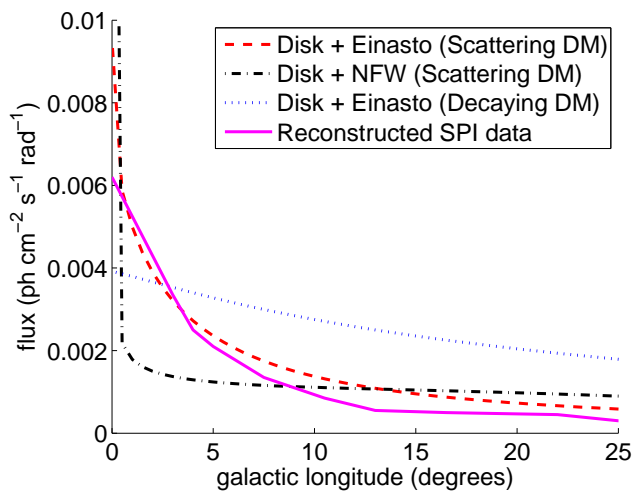


Figure 2: Longitudinal dark matter profiles for the three dark matter models considered, including the disk component from radioactive isotopes. Fluxes are integrated over galactic latitudes $-15^\circ < b < 15^\circ$. “Scattering” refers to either scattering multistate dark matter or annihilating light dark matter. The solid magenta line is left-right averaged, reconstructed SPI data from [6], taken from the skymaps of [37].

matter. The scattering scenario provided a consistently better fit ($\Delta\text{MLR} > 400$), and the fit to the Einasto profile was significantly better than to the NFW profile ($\Delta\text{MLR} = 513$). Motivated by the triaxial halo shapes mentioned above [27], we also examined an oblate Einasto profile with a semi-major axis ratio $c/a = 0.8$. This is denoted “Einasto (oblate) + disk” in Table I. While this reduced the required flux from the disk component, it did not produce any significant change in MLR.

The best-fit lifetimes (cross-sections) of the XDM model in the decaying (scattering) scenario are presented in the final column of Table I. Figure 1 shows the all-sky map of the Einasto + disk best fit to the INTEGRAL/SPI data, and Figure 2 shows the longitudinal profile of the three dark matter models (including disk

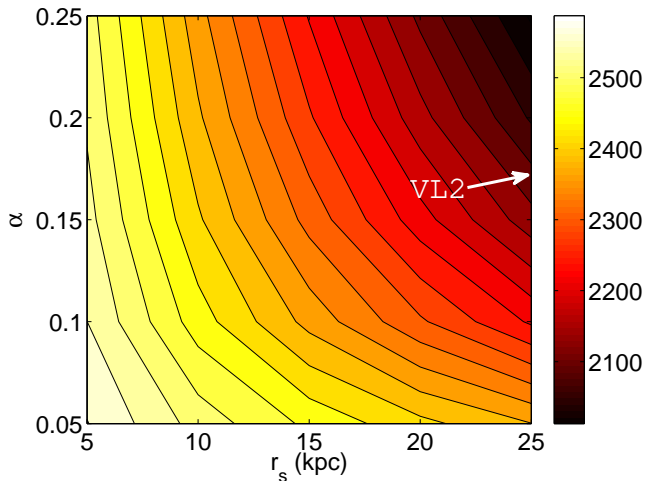


Figure 3: Maximum log-likelihood ratio (MLR) obtained in the decaying dark matter + young disk scenario as a function of the Einasto halo parameters. The values favored by the *Via Lactea II* N-body simulation, labeled *VL2*, do not give a good fit to the INTEGRAL/SPI data and are far away from the favored region.

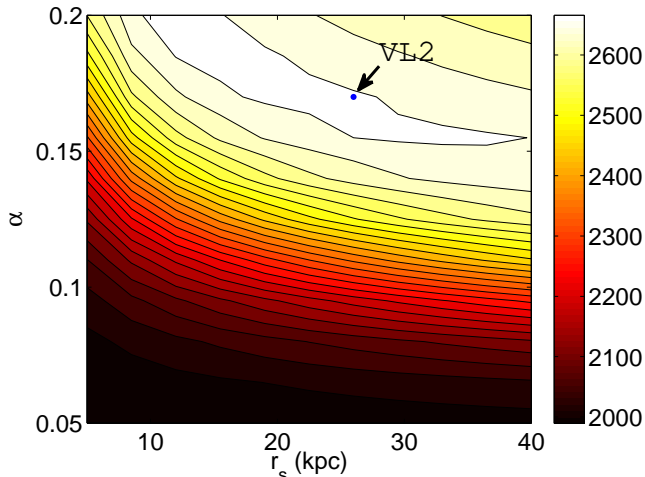


Figure 4: Same as Figure 3, but with scattering dark matter (4). The MLR obtained with the *Via Lactea II* parameters (white dot) is within $\Delta MLR = 5$ of the best fit ($r_s = 12$ kpc, $\alpha = 0.2$), which means that the VL2 parameters likely correspond to the correct model if the scattering or annihilating dark matter hypothesis is true.

components) in comparison with a reconstruction of the SPI data. This clearly illustrates how decaying dark matter produces a profile that is far too flat, while an NFW distribution results in an unrealistic sharp central peak. Decaying dark matter in an NFW profile (not illustrated) displays a combination of these flaws. On the other hand, the scattering model produces $MLR = 2668$, which is not far below that of the best-fit phenomenological model, the latter having $MLR = 2693$ and six additional fitting

parameters. The reduced χ^2 of our dark matter model computed on a pointing basis is as good as that of the phenomenological model, with a value of 1.007.

Letting r_s , α and z_0 vary freely yields some improvement. Figure 3 shows a contour plot of the MLR obtained from the decay scenario (3). The favored region in the lower-left corner, with an MLR of 2558, corresponds to an extremely cuspy DM halo that is quite far removed from realistic DM halo models.

The equivalent picture for scattering DM is illustrated in Figure 4. The overall best fit was found to be for a profile with $\alpha = 0.2$, $r_s = 12$ kpc and $z_0 = 140$ pc, with an MLR of 2673. However, this difference is only marginally significant. Indeed, by adding three degrees of freedom, such an improvement should happen by chance 17% of the time due to statistical fluctuations in the data. We found that the young disk (YD) model consistently gave a better fit than the old disk (OD) model, and that adjusting z_0 over a range from 70 to 200 pc did not produce any significant improvement in the MLR. Finally, we checked that choosing a closer value for the galactocentric distance of $R = 8.2$ kpc, as suggested by recent studies such as [30] produced a negligible change in the fit ($\Delta MLR < 1$).

6. DISCUSSION AND CONCLUSION

We have made the first direct comparison of dark matter predictions for the observed 511 keV spatial intensity distribution since the earliest data release of INTEGRAL/SPI. Our favored fit corresponds to a scattering excited DM or annihilating light DM model in an Einasto density distribution (1) with parameters fixed to the *Via Lactea II* results. We confirm previous analyses showing that decaying dark matter is ruled out due to its too-broad spatial distribution. After correct normalization of the intensity, our best-fit model requires a cross section for $\chi\chi$ to produce positrons of $\langle\sigma v\rangle_\chi = 5.1 \times 10^{-25} (m_\chi/\text{GeV})^2 \text{ cm}^3\text{s}^{-1}$. If m_χ is in the 10-1000 GeV range as favored by most WIMP models, this means $\langle\sigma v\rangle$ is in the interval $[10^{-23}, 10^{-19}] \text{ cm}^3\text{s}^{-1}$. The fact that this is far above the annihilation cross section of $3 \times 10^{-26} \text{ cm}^3\text{s}^{-1}$ needed to get the observed relic density is not problematic, because the physical process required in these models is inelastic scattering to an excited state rather than annihilation.

Because we neglected r -dependence in the averaged cross section $\langle\sigma v\rangle$, these results apply to upscattering XDM with high masses $m_\chi \gtrsim$ a few TeV, metastable XDM models [16, 17], and direct annihilation of MeV DM. To cover the case of lighter XDM models, a more detailed analysis taking account of the radial dependence of the DM velocity dispersion in the Galaxy would be needed. We hope to return to this in future work.

For light \sim MeV DM annihilating directly into e^+e^- , our required cross section is $\langle\sigma v\rangle \sim 10^{-31} \text{ cm}^3\text{s}^{-1}$, which is too small to give the right relic density. This need

not be a problem; it only requires there to be additional stronger annihilation channels into invisible particles, for example dark gauge bosons [35] or dark neutrinos [38].

There are two unknowns that could change our analysis in significant ways. One is the distance by which positrons propagate between creation and annihilation. If it is larger than ~ 100 pc, it could alter the overall breadth of the spatial extent of the signal, as well as introduce deviations from axial symmetry, depending on the conditions of the interstellar medium in the bulge. Further observational evidence constraining the structure of magnetic fields (for example synchrotron emission studies [39]) will be needed to reduce these uncertainties. A second unknown is the degree of departure of the DM halo from spherical symmetry, which definitely occurs in N -body simulations [27]. We showed that adding some oblateness had little effect on the fits, though the nature and extent of triaxiality near the galactic center depends heavily upon the inclusion of baryons in the simulations, a challenging field which is still in its early stages. We look forward to improvements in these studies that will help to constrain the theoretically expected extent of triaxiality in the DM halo.

We have confirmed the findings of previous studies concerning the disk emission. Given a young disk model for the distribution of ^{26}Al , the observed flux of 1809 keV gamma rays [23] translates into an expected 511 keV flux of $(7.33 \pm 0.89) \times 10^{-4}$ ph cm $^{-2}$ s $^{-1}$. This alone accounts for 73% of the disk component favored by our model. If similar amounts of ^{44}Ti are present in the Galaxy, there is no need for an extra component to explain the disk component of the 511 keV signal. On the other hand, simulations show that in addition to the DM halo, there may also be a DM disk. This would give an extra DM contribution to the disk component of the 511 keV emission. However, there is as yet no direct evidence for a

DM disk in our own galaxy [40, 41].

It is worth emphasizing that only two degrees of freedom were required to obtain the MLR of 2668 in the DM scattering/annihilation scenario. This is in contrast to the 8 d.o.f. necessary to obtain an MLR of 2693 with one best-fit phenomenological model. A further advantage of the DM model is that it is motivated by particle physics and cosmology, and it has a concrete, calculable production mechanism for the excess electron-positron pairs. Our results are independent of the details of the DM model, so long as the scattering events lead directly to an e^+e^- pair.

We find these results to be encouraging for the dark matter interpretation of the 511 keV excess, an anomaly that was first seen in 1972 by balloon-borne detectors [42]. We hope that the experimental hard X-ray / soft gamma-ray astronomy community will be motivated to consider a higher-resolution instrument that would be sensitive to the 511 keV region of the spectrum in the future. Such observations would help to shed more light on this intriguing possibility, which could be the first evidence for nongravitational interactions of dark matter.

Acknowledgments

We thank the anonymous referee for insightful comments that helped to improve our presentation. We would like to thank Evan McDonough for his contributions to our skymap models. JC is supported by NSERC (Canada). PM acknowledges support from the European Community via contract ERC-StG-200911, and ACV is supported by an NSERC Alexander Graham Bell Canada Graduate Scholarship.

-
- [1] J. Knodlseder *et al.*, *Astron. Astrophys.* **441**, 513 (2005), astro-ph/0506026.
 - [2] E. Churazov, R. Sunyaev, S. Sazonov, M. Revnivtsev, and D. Varshalovich, *Mon.Not.Roy.Astron.Soc.* **357**, 1377 (2005), astro-ph/0411351.
 - [3] P. Jean *et al.*, *Astron.Astrophys.* **445**, 579 (2006), astro-ph/0509298.
 - [4] J. F. Beacom and H. Yuksel, *Phys.Rev.Lett.* **97**, 071102 (2006), astro-ph/0512411.
 - [5] R. M. Bandyopadhyay, J. Silk, J. E. Taylor, and T. J. Maccarone, (2008), 0810.3674.
 - [6] N. Prantzos *et al.*, (2010), 1009.4620.
 - [7] C. Boehm, D. Hooper, J. Silk, M. Casse, and J. Paul, *Phys.Rev.Lett.* **92**, 101301 (2004), astro-ph/0309686.
 - [8] D. P. Finkbeiner and N. Weiner, *Phys.Rev.* **D76**, 083519 (2007), astro-ph/0702587.
 - [9] M. Pospelov and A. Ritz, *Phys.Lett.* **B651**, 208 (2007), hep-ph/0703128.
 - [10] N. Arkani-Hamed, D. P. Finkbeiner, T. R. Slatyer, and N. Weiner, *Phys.Rev.* **D79**, 015014 (2009), 0810.0713.
 - [11] PAMELA Collaboration, O. Adriani *et al.*, *Nature* **458**, 607 (2009), 0810.4995.
 - [12] The Fermi LAT Collaboration, A. A. Abdo *et al.*, *Phys.Rev.Lett.* **102**, 181101 (2009), 0905.0025.
 - [13] R. Bernabei *et al.*, *Eur.Phys.J.* **C67**, 39 (2010), 1002.1028.
 - [14] F. Chen, J. M. Cline, A. Fradette, A. R. Frey, and C. Rabideau, *Phys.Rev.* **D81**, 043523 (2010), 0911.2222.
 - [15] R. Morris and N. Weiner, (2011), 1109.3747.
 - [16] F. Chen, J. M. Cline, and A. R. Frey, *Phys.Rev.* **D79**, 063530 (2009), 0901.4327.
 - [17] J. M. Cline, A. R. Frey, and F. Chen, *Phys.Rev.* **D83**, 083511 (2011), 1008.1784.
 - [18] Y. Ascasibar, P. Jean, C. Boehm, and J. Knodlseder, *Mon.Not.Roy.Astron.Soc.* **368**, 1695 (2006), astro-ph/0507142.
 - [19] Z. Abidin, A. Afanasev, and C. E. Carlson, (2010), 1006.5444.
 - [20] G. Weidenspointner *et al.*, (2007), astro-ph/0702621.
 - [21] G. Weidenspointner *et al.*, *New Astronomy Reviews* **52**,

- 454 (2008).
- [22] L. Bouchet, J.-P. Roques, and E. Jourdain, *Astrophys.J.* **720**, 1772 (2010), 1007.4753.
- [23] R. Diehl *et al.*, *Astron.Astrophys.* **449**, 1025 (2006), astro-ph/0512334.
- [24] K.-W. Chan and R. E. Lingenfelter, *Astrophys. J.* **405**, 614 (1993).
- [25] P. Martin, J. Vink, S. Jiraskova, P. Jean, and R. Diehl, (2010), 1006.2537.
- [26] C. A. Vera-Ciro *et al.*, (2011), 1104.1566.
- [27] P. B. Tissera, S. D. White, S. Pedrosa, and C. Scannapieco, (2009), 0911.2316.
- [28] J. Diemand *et al.*, *Nature* **454**, 735 (2008), 0805.1244.
- [29] M. Kuhlen, P. Madau, and J. Silk, *Science* **325**, 970 (2009), 0907.0005.
- [30] P. Salucci, F. Nesti, G. Gentile, and C. Martins, *Astron.Astrophys.* **523**, A83 (2010), 1003.3101.
- [31] F. J. Kerr and D. Lynden-Bell, *Mon.Not.Roy.Astron.Soc.* **221**, 1023 (1986).
- [32] C. Picciotto and M. Pospelov, *Phys.Lett.* **B605**, 15 (2005), hep-ph/0402178.
- [33] J. Higdon, R. Lingenfelter, and R. Rothschild, *Astrophys.J.* **698**, 350 (2009), 0711.3008.
- [34] P. Jean, W. Gillard, A. Marcowith, and K. Ferriere, (2009), 0909.4022.
- [35] J.-H. Huh, J. E. Kim, J.-C. Park, and S. C. Park, *Phys.Rev.* **D77**, 123503 (2008), 0711.3528.
- [36] A. C. Robin, C. Reyle, S. Derriere, and S. Picaud, *Astron.Astrophys.* **409**, 523 (2003), astro-ph/0401052.
- [37] G. Weidenspointner *et al.*, *Nature* **451**, 159 (2008).
- [38] J. M. Cline and A. R. Frey, *Phys.Lett.* **B706**, 384 (2012), 1109.4639.
- [39] T. Bringmann, F. Donato, and R. A. Lineros, (2011), 1106.4821.
- [40] C. Bidin, G. Carraro, R. Mendez, and W. van Altena, *Astrophys.J.* **724**, L122 (2010), 1011.1289.
- [41] J. L. G. Pestana and D. H. Eckhardt, *Astrophys.J.* **722**, L70 (2010), 1009.0925.
- [42] W. N. Johnson III, F. R. Harnden Jr., and R. C. Haymes, *Astrophys.J.* **172**, L1 (1979).